



The Manganese-Dependent Pyruvate Kinase PykM Is Required for Wild-Type Glucose Utilization by *Brucella abortus* 2308 and Its Virulence in C57BL/6 Mice

Joshua E. Pitzer,^a Tonya N. Zeczycki,^b John E. Baumgartner,^{a*} Daniel W. Martin,^a R. Martin Roop II^a

^aDepartment of Microbiology and Immunology, Brody School of Medicine, East Carolina University, Greenville, North Carolina, USA

^bDepartment of Biochemistry and Molecular Biology, Brody School of Medicine, East Carolina University, Greenville, North Carolina, USA

ABSTRACT Pyruvate kinase plays a central role in glucose catabolism in bacteria, and efficient utilization of this hexose has been linked to the virulence of *Brucella* strains in mice. The brucellae produce a single pyruvate kinase which is an ortholog of the *Bradyrhizobium* manganese (Mn)-dependent pyruvate kinase PykM. A biochemical analysis of the *Brucella* pyruvate kinase and phenotypic analysis of a *Brucella abortus* mutant defective in high-affinity Mn import indicate that this enzyme is an authentic PykM ortholog which functions as a Mn-dependent enzyme *in vivo*. The loss of PykM has a negative impact on the capacity of the parental 2308 strain to utilize glucose, fructose, and galactose but not on its ability to utilize ribose, xylose, arabinose, or erythritol, and a *pykM* mutant displays significant attenuation in C57BL/6 mice. Although the enzyme pyruvate phosphate dikinase (PpdK) can substitute for the loss of pyruvate kinase in some bacteria and is also an important virulence determinant in *Brucella*, a phenotypic analysis of *B. abortus* 2308 and isogenic *pykM*, *ppdK*, and *pykM ppdK* mutants indicates that PykM and PpdK make distinctly different contributions to carbon metabolism and virulence in these bacteria.

IMPORTANCE Mn plays a critical role in the physiology and virulence of *Brucella* strains, and the results presented here suggest that one of the important roles that the high-affinity Mn importer MntH plays in the pathogenesis of these strains is supporting the function of the Mn-dependent kinase PykM. A better understanding of how the brucellae adapt their physiology and metabolism to sustain their intracellular persistence in host macrophages will provide knowledge that can be used to design improved strategies for preventing and treating brucellosis, a disease that has a significant impact on both the veterinary and public health communities worldwide.

KEYWORDS *Brucella*, glucose catabolism, manganese, pyruvate kinase

The members of the genus *Brucella* are Gram-negative bacteria that predominantly cause abortion and infertility in their natural mammalian hosts (1). *Brucella melitensis*, *Brucella abortus*, and *Brucella suis* are also important human pathogens in areas of the world where the corresponding infections are not controlled in food animals (2). Like most other bacteria, *Brucella* strains require certain metals as micronutrients to support their cellular physiology (3). The ability to meet their physiologic need for some of these micronutrients is particularly challenging for the brucellae, because in addition to having to scavenge often limited concentrations of these metals from the external environment, these bacteria also have to overcome the so-called “metal-withholding” defenses that are part of the innate and acquired immune responses of their mammalian hosts (4).

Manganese (Mn) is an essential micronutrient for some bacteria during routine

Received 2 August 2018 Accepted 18 September 2018

Accepted manuscript posted online 1 October 2018

Citation Pitzer JE, Zeczycki TN, Baumgartner JE, Martin DW, Roop RM, II. 2018. The manganese-dependent pyruvate kinase PykM is required for wild-type glucose utilization by *Brucella abortus* 2308 and its virulence in C57BL/6 mice. *J Bacteriol* 200:e00471-18. <https://doi.org/10.1128/JB.00471-18>.

Editor George O'Toole, Geisel School of Medicine at Dartmouth

Copyright © 2018 American Society for Microbiology. All Rights Reserved.

Address correspondence to R. Martin Roop II, roopr@ecu.edu.

* Present address: John E. Baumgartner, Office of Prospective Health, Brody School of Medicine, East Carolina University, Greenville, North Carolina, USA.

in vitro cultivation (5), but for others, this metal only appears to be required when the bacteria are subjected to an environmental stress, such as an exposure to reactive oxygen species (ROS) (6). Mn-dependent superoxide dismutases such as SodA, for instance, are important cytoplasmic antioxidants in bacteria (7), and in some cases, bacteria can substitute Mn for Fe in cellular proteins that do not require the redox activity of the latter metal for their function as a means of protecting these proteins from damage mediated by ROS via Fenton chemistry (6).

Brucella strains produce a single high-affinity Mn transporter, MntH, and a phenotypic analysis of an isogenic *mntH* mutant derived from *B. abortus* 2308 indicates that Mn plays an important role in the basic physiology of these bacteria (8). The *B. abortus* *mntH* mutant, for instance, displays delayed growth compared to that of the parental strain during liquid culture in both a Mn-deprived minimal medium and a more complex medium (e.g., brucella broth). This mutant also produces smaller colonies on Schaedler blood agar that take longer to develop than those produced by 2308 (9). The growth defects displayed by the *B. abortus* *mntH* mutant can be alleviated by supplementing these culture media with Mn but not with other divalent cations such as Fe, Zn, Cu, Co, or Ni (8). This basal requirement of *Brucella* strains for Mn was reported previously (10) and is a characteristic that is shared with at least some of the other alphaproteobacteria, including *Sinorhizobium meliloti* (11), *Bradyrhizobium japonicum* (5), and *Agrobacterium tumefaciens* (12). In the case of *B. japonicum*, the activities of two Mn-dependent enzymes, the superoxide dismutase SodM and the pyruvate kinase PykM, have been found to contribute significantly to the basal requirement of this bacterium for Mn during routine *in vitro* cultivation (5). *Brucella* strains also produce a Mn-dependent superoxide dismutase, SodA, which serves as an important antioxidant (13), and a *B. abortus* *mntH* mutant is deficient in SodA activity (8). Like its *mntH* counterpart, an isogenic *B. abortus* *sodA* mutant displays a prominent growth defect during *in vitro* cultivation, which suggests that supporting SodA activity also represents an important component of the basal requirement of *Brucella* strains for Mn.

In addition to its distinctive *in vitro* phenotype, the *B. abortus* *mntH* mutant also displays severe attenuation in cultured murine macrophages and experimentally infected mice (8). Mn-dependent superoxide dismutases (SODs) have been linked to the virulence of several bacteria, including *Brucella* (13–17), and it has been proposed that inhibiting the activities of these enzymes plays an important role in the protective capacity of the host metal-binding protein calprotectin (18). However, a comparison of the attenuation profiles of isogenic *B. abortus* *sodA* and *mntH* mutants in mice clearly shows that Mn plays a much more extensive role in the virulence of *Brucella* strains than simply supporting their SodA activity (8, 13).

The recent discovery of the Mn dependence of the *Bradyrhizobium japonicum* pyruvate kinase PykM offers another possible explanation for the importance of Mn for the virulence of *Brucella* strains. Specifically, studies by Xavier et al. (19) have shown that glucose catabolism plays a critical role in the capacity of *B. abortus* 2308 to sustain chronic spleen infections in experimentally infected mice. Because they lack the enzyme phosphofructokinase (20), *Brucella* strains cannot catabolize this sugar using the Embden-Meyerhof-Parnas pathway. Instead, they rely on the pentose phosphate pathway for glucose catabolism (20–22). Pyruvate kinase catabolizes an important step in the latter stages of glucose catabolism via this pathway, and thus, it is notable that the sole pyruvate kinase produced by *Brucella* strains is an ortholog of the Mn-dependent enzyme PykM. The studies described in this report were performed to evaluate the biochemical properties and metal dependence of the *Brucella* PykM and assess its contribution to glucose catabolism and virulence.

RESULTS

Mn is the preferred metal cofactor for the *Brucella* pyruvate kinase. A survey of the *Brucella* genome sequences currently available in GenBank indicated that these bacteria produce a single pyruvate kinase. The gene encoding this enzyme in the *B. abortus* 2308 genome is designated BAB1_1761, and the corresponding gene product

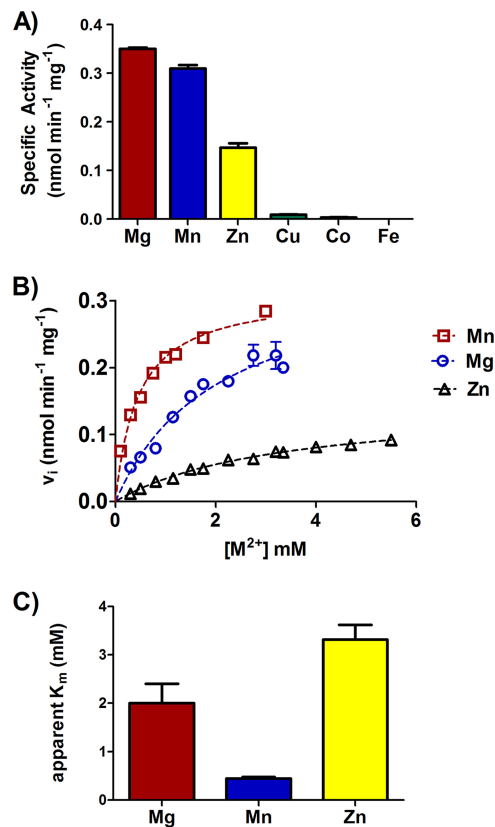


FIG 1 Specific activity (A), kinetics (B), and apparent K_m (C) of the *Brucella* PykM in a pyruvate kinase assay with different metals as cofactors. Each data point represents the mean and standard deviation from four different experiments.

is predicted to be a 478-amino acid protein that shares 64% identity and 80% similarity with the *Bradyrhizobium* pyruvate kinase PykM. The latter protein is somewhat atypical compared to many other bacterial pyruvate kinases that have been described, because it requires Mn instead of Mg to support its enzymatic activity and its activity is not regulated by the allosteric activators fructose-1,6-bis-phosphate (FBP) or AMP (5).

To determine if the *Brucella* PykM ortholog has biochemical properties similar to those described for its *Bradyrhizobium* counterpart, a recombinant version of the *Brucella* protein was examined in a pyruvate kinase assay (Fig. 1). Mg, Mn, or Zn supported the enzymatic activity of the *Brucella* pyruvate kinase in this assay (Fig. 1A), but the specific activity obtained with Zn was considerably lower than that obtained when Mg or Mn was used in the assay. However, Mn appears to be the preferred cofactor for the *Brucella* pyruvate kinase, because the apparent K_m (0.45 ± 0.03 mM) obtained for this enzyme with Mn in the reaction mixture was significantly lower than that obtained when Mg (2.1 ± 0.4 mM) or Zn (3.3 ± 0.3 mM) was used (Fig. 1B and C). The preference of the *Brucella* pyruvate kinase for Mn is further supported by the observation that the total cellular pyruvate kinase activity measured in a *B. abortus* mutant lacking the high-affinity Mn importer MntH (8) was significantly lower than that detected in the parental strain when these strains were grown under Mn-depleted conditions (Fig. 2). Notably, this same dependence upon MntH to support its function is a distinctive feature of the *Bradyrhizobium* PykM (5). It was also found that the addition of FBP or AMP to the reaction mixture did not influence the enzymatic activity of the *Brucella* protein in the pyruvate kinase assay (data not shown). On the basis of these findings, we propose that the *Brucella* pyruvate kinase is an authentic PykM ortholog that functions as a Mn-dependent enzyme *in vivo*.

A *pykM* mutation negatively impacts the ability of *B. abortus* 2308 to utilize glucose, fructose, and galactose. With the exception of the fact that it produces

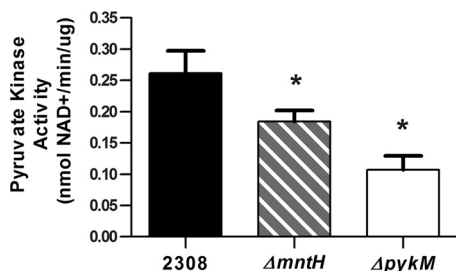


FIG 2 Pyruvate kinase activity in *B. abortus* 2308 and $\Delta mntH$ and $\Delta pykM$ mutant cells grown to mid-log phase in a Mn-restricted defined medium. The data represent the results of 3 assays performed at different times. The baseline levels of NADH to NAD conversion in reaction mixtures not containing cell lysate or PEP have been subtracted from the values presented. *, $P < 0.05$ for comparisons of 2308 versus the *mntH* and *pykM* mutants by least significant difference one-way analysis of variance (LSD-ANOVA).

slightly smaller colonies than the parental 2308 strain when grown on Schaedler agar supplemented with blood, the *B. abortus pykM* mutant JEP2 otherwise displayed wild-type growth in rich media, including brucella broth and Trypticase soy broth. However, as reported previously by Gao et al. (23) the *B. abortus pykM* mutant did exhibit a significant growth defect when grown in the minimal medium described by this group supplemented with glucose, and importantly, this growth defect was rescued by the addition of pyruvate to the medium (Fig. 3).

The coding regions of *pykM* and the upstream gene *bab1_1762*, annotated in the *B. abortus* 2308 genome sequence, overlap by 3 bp, and a transcriptional analysis indicated that these genes are transcribed as an operon (data not shown). When a DNA fragment containing *pykM* and the upstream gene was cloned into pMR10 (24), the resulting plasmid produced an aberrant growth phenotype in the *pykM* mutant. Consequently, we elected to “reconstruct” the wild-type version of the *pykM* gene in *B. abortus pykM* mutant JEP2 to confirm the link between the *pykM* mutation and the phenotype exhibited by this mutant. As shown in Fig. 3, the derivative of JEP2 with the reconstructed *pykM* gene (JEP31) displayed wild-type growth in minimal medium supplemented with glucose.

To determine if the *pykM* mutation affects the capacity of *B. abortus* to utilize sugars other than glucose, we examined the capacity of *B. abortus* 2308 and the *pykM* mutant to utilize glucose, galactose, fructose, ribose, L-arabinose, and xylose using Biolog phenotypic microarray plates. These are the major sugars reported to be used by *B. abortus* strains (25, 26), and glucose catabolism has been experimentally linked to the virulence of strain 2308 in mice (19). As shown in Fig. 4, the *B. abortus pykM* mutant displayed a significant reduction in its capacity to utilize glucose, fructose, and galactose compared to that of the parent strain and the *B. abortus* mutant with the reconstructed *pykM* locus. In contrast, *B. abortus* 2308, the *pykM* mutant, and the *B. abortus* mutant with the reconstructed *pykM* locus displayed the same levels of xylose, ribose, and L-arabinose utilization (Fig. 4).

The results presented in Fig. 4 indicate that *Brucella* strains are like many other bacteria and have evolved alternative enzymatic pathways that enable them to bypass an absolute need for pyruvate kinase during carbohydrate catabolism. One enzyme that would conceivably enable them to do this is pyruvate phosphate dikinase (PpdK) (27). This enzyme ordinarily catalyzes the conversion of pyruvate to phosphoenolpyruvate (PEP) during gluconeogenesis but can also carry out the reverse reaction, and some bacteria use PpdK to compensate for the absence of pyruvate kinase (28, 29). To determine to what extent PpdK contributes to carbohydrate catabolism in the presence or absence of PykM, we evaluated the carbohydrate utilization patterns of *B. abortus* 2308 and isogenic *pykM*, *ppdK*, and *pykM ppdK* mutants in the Biolog plates. As shown in Fig. 5, the *B. abortus ppdK* mutant displayed the same utilization profiles as the parental 2308 strain for all of the carbohydrates examined (including erythritol), and the introduction of a *ppdK* mutation into the *pykM* mutant did not enhance the defect in

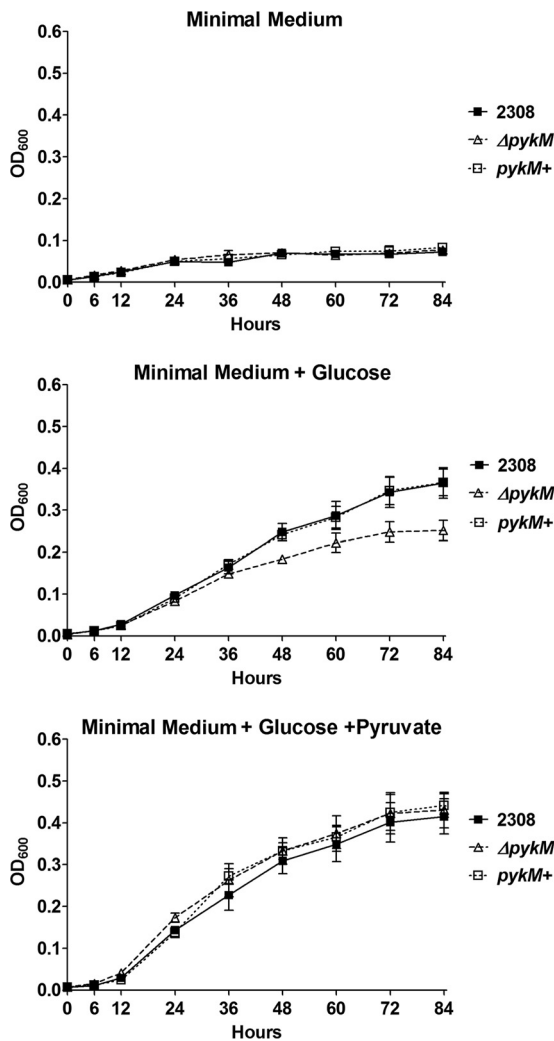


FIG 3 Growth kinetics of *B. abortus* 2308, the isogenic $\Delta pykM$ mutant JEP2, and a derivative of JEP2 in which the *pykM* locus has been reconstructed (*pykM*⁺) (JEP31) in minimal medium, minimal medium containing 55 mM glucose, and minimal medium containing 55 mM glucose and 55 mM pyruvate. The data represent the means and standard deviations from three separate cultures for each strain under each experimental condition examined in a single experiment. This experiment was repeated three times with the same results.

glucose, fructose, or galactose utilization exhibited by this mutant. These experimental findings indicate that PpdK does not compensate for the loss of PykM activity during carbohydrate catabolism in *B. abortus* 2308.

The Entner-Doudoroff (ED) pathway is another mechanism by which bacteria can bypass the pyruvate kinase reaction during the catabolism of hexoses such as glucose, fructose, and galactose (30). This pathway employs the enzymes 6-phosphogluconate dehydratase (Edd) and 2-keto-3-deoxy-6-phosphogluconate aldolase (Eda) to convert 6-phosphogluconate, an intermediate of hexose catabolism via the pentose phosphate pathway, to pyruvate and glyceraldehyde-3-phosphate. Although *Brucella* strains possess the genetic capacity to utilize the ED pathway, *B. abortus* strains typically do not use it (22). However, the possibility exists that these strains can redirect carbon flow through this pathway during the catabolism of hexoses if they lack a functional pyruvate kinase. Moreover, if this redirection results in a diminished capacity of the *pykM* mutant to catabolize hexoses, this might explain why this mutant displays reduced utilization of glucose, fructose, and galactose compared to that of the parent strain. To determine if the ED pathway contributes to hexose catabolism in the *B.*

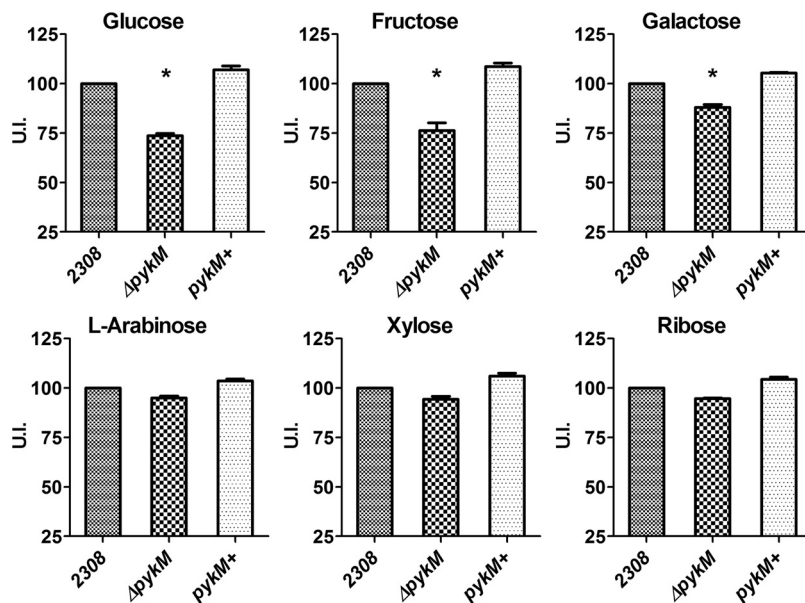


FIG 4 Capacity of *B. abortus* 2308, JEP2 ($\Delta pykM$) and JEP31 ($pykM^+$) to utilize selected carbohydrates in a Biolog phenotypic microarray assay. The utilization index (U.I.) was calculated as described in Materials and Methods. The data presented are the means and standard deviations of the results obtained from single determinations made in three different experiments. *, $P < 0.05$ for comparisons of 2308 versus the $pykM$ mutant by LSD-ANOVA.

abortus pykM mutant, *B. abortus* 2308 and isogenic $pykM$, *edd*, and $pykM edd$ mutants were assessed for their ability to utilize glucose, fructose, galactose, and other carbohydrates in the Biolog plates (Fig. 6). Similar to what was observed with the $ppdK$ mutants, the *B. abortus edd* mutant displayed the same carbohydrate utilization patterns as the parental 2308 strain, and the *edd* mutation did not enhance the defect in glucose, fructose, or galactose utilization observed in the *B. abortus pykM* mutant. Thus, the redirection of hexose catabolism through the ED pathway does not explain the negative impact that the $pykM$ mutation has on the utilization of these sugars in *B. abortus* 2308.

To account for the possibility that the presence of either PpdK or the ED pathway enables the *B. abortus pykM* mutant to sustain carbon flow during carbohydrate catabolism, we constructed *B. abortus ppdK edd* and $pykM ppdK edd$ mutants and compared the carbohydrate utilization patterns of these strains with those of the parental 2308 strain and the $pykM$ mutant. As shown in Fig. 7, the *B. abortus ppdK edd* mutant displayed the same carbohydrate utilization pattern as *B. abortus* 2308, and the $pykM ppdK edd$ mutant exhibited the same carbohydrate utilization pattern as the $pykM$ mutant.

PykM and PpdK make independent contributions to the virulence of *B. abortus* 2308 in mice. The data presented here and elsewhere (23, 27) strongly suggest that the pyruvate kinase PykM and pyruvate phosphate dikinase PpdK make different contributions to glucose metabolism in *Brucella*, with PykM being required for wild-type catabolism of this sugar and PpdK being needed for its synthesis from gluconeogenic substrates. Both of these enzymes are required for the wild-type virulence of *B. abortus* 2308 in BALB/c mice (23, 27). To gain further insight into the relative contributions of PykM and PpdK to virulence, we assessed the capacity of *B. abortus* 2308 and isogenic $pykM$, $ppdK$, and $pykM ppdK$ mutants to establish and maintain chronic spleen infections in C57BL/6 mice, another mouse strain that is widely used for virulence testing in *Brucella*. Consistent with earlier reports, the *B. abortus pykM* and $ppdK$ mutants also display significant attenuation compared to 2308 in the C57BL/6 mice (Fig. 8). But more importantly, the $pykM ppdK$ double mutant exhibited significantly increased attenuation in these mice compared to either of the $pykM$ or $ppdK$ single mutant parent strains,

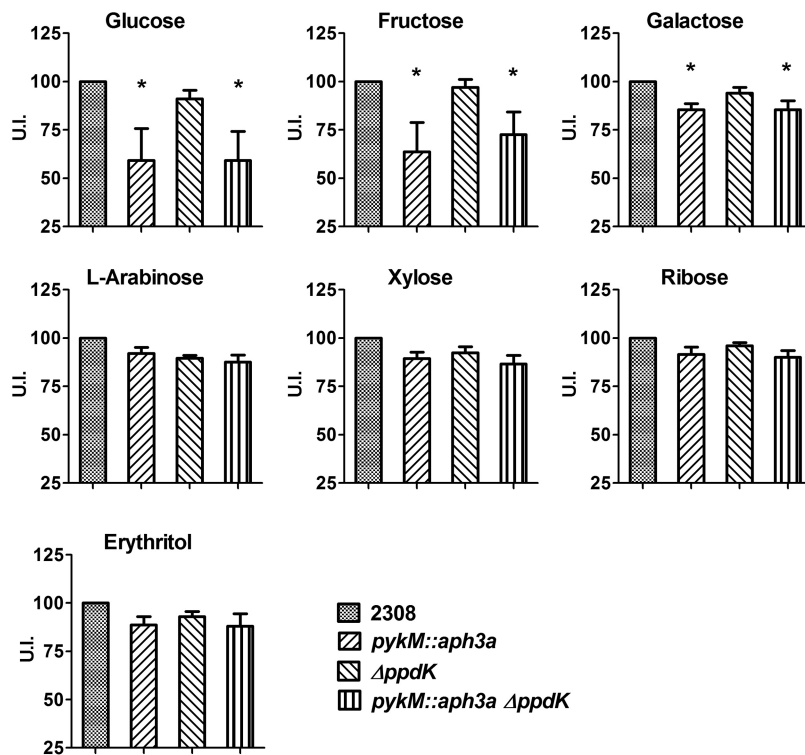


FIG 5 Carbohydrate utilization profiles of *B. abortus* 2308 and isogenic *pykM::aph3a*, $\Delta ppdK$, and *pykM::aph3a* $\Delta ppdK$ mutants. The U.I. was calculated as described in Materials and Methods. The data presented are the means and standard deviations of the results obtained from single determinations made in three different experiments. *, $P < 0.05$ for comparisons of 2308 versus the *pykM::aph3a* and *pykM::aph3a* $\Delta ppdK$ mutants by LSD-ANOVA.

which strongly suggests that the corresponding enzymes make separate and independent contributions to virulence, which is consistent with them performing different physiologic functions.

DISCUSSION

The studies reported here show that the sole pyruvate kinase produced by *Brucella* strains is a functional ortholog of the *Bradyrhizobium* Mn-dependent pyruvate kinase PykM (5), and that this enzyme plays an important role in glucose, fructose, and galactose catabolism in *B. abortus* 2308. They also confirm and extend the results initially reported by Gao et al. (23) that PykM is required for the wild-type virulence of this strain in the mouse model of chronic infection. Pyruvate kinase has been linked to the virulence of other bacterial pathogens (31, 32), but this link in *Brucella* is especially notable for two reasons. The first is that the data presented here suggest that one of the reasons that the high-affinity Mn importer MntH plays such an important role in the virulence of *Brucella* strains (8) is that it enables them to acquire enough Mn to support PykM activity in the Mn-deprived environment they encounter in their mammalian hosts (4). The second is that the link between PykM and glucose catabolism in *B. abortus* 2308 offers further support for the proposition that glucose catabolism plays a critical role in the virulence of *Brucella* strains in the mouse model (19).

Another important observation is that except for its effect on glucose, fructose, and galactose utilization, the *pykM* mutation had no significant impact on the capacity of *B. abortus* 2308 to utilize any of the other carbohydrates examined in this study. This is an intriguing and potentially informative finding when one considers what is currently known about the carbohydrate metabolism pathways in *Brucella* (22). These bacteria catabolize carbohydrates via the pentose phosphate pathway, and pyruvate kinase plays an essential role in maintaining carbon flow through this pathway and into the

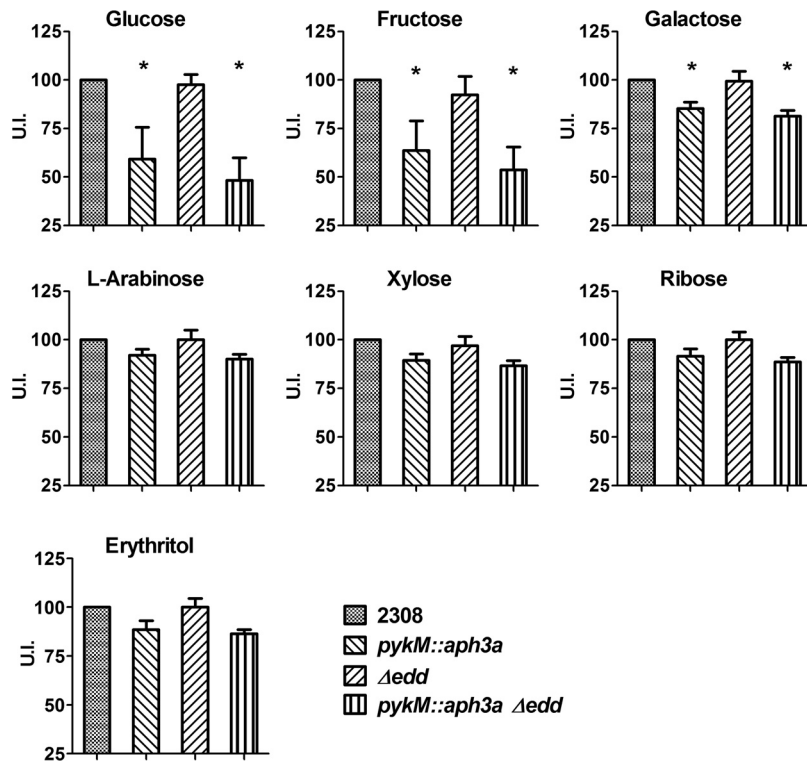


FIG 6 Carbohydrate utilization profiles of *B. abortus* 2308 and isogenic *pykM::aph3a*; Δ *edd*; and *pykM::aph3a* Δ *edd* mutants. The U.I. was calculated as described in Materials and Methods. The data presented are the means and standard deviations of the results obtained from single determinations made in three different experiments. *, $P < 0.05$ for comparisons of 2308 versus the *pykM::aph3a* and *pykM::aph3a* Δ *edd* mutants by LSD-ANOVA.

tricarboxylic acid (TCA) cycle unless the cell has alternative mechanisms for converting PEP to pyruvate. An obvious candidate for catalyzing the direct conversion of PEP to pyruvate during carbohydrate catabolism in the absence of pyruvate kinase is the enzyme pyruvate phosphate dikinase (PpdK). Ordinarily, PpdK catalyzes the conversion of pyruvate to PEP during gluconeogenesis in bacteria, and Zúñiga-Ripa et al. (27) have provided convincing evidence that PpdK performs this function in *B. abortus* 2308. However, PpdK can also convert PEP to pyruvate in bacterial strains that lack a pyruvate kinase (28, 29), and the background level of PEP to pyruvate conversion by the *B. abortus* *pykM* mutant observed in this study (Fig. 2) suggests that the *Brucella* PpdK can also carry out this reaction. However, a *ppdK* mutation did not diminish the capacity of the *B. abortus* *pykM* mutant JEP2 to catabolize ribose, arabinose, xylose, or erythritol or further diminish the ability of this mutant to utilize glucose, fructose, or galactose, which indicates that PpdK is not compensating for the loss of pyruvate kinase activity in the *pykM* mutant during catabolism of these carbohydrates. This is a particularly relevant finding, because it suggests that PykM and PpdK play distinctly different roles in glucose metabolism, with PykM being involved in the catabolism of this hexose and PpdK being required for its biosynthesis from gluconeogenic substrates (30). Bacteria can also employ the anaplerotic enzyme PEP carboxylase to convert PEP to pyruvate by an indirect route when pyruvate kinase is absent (33), but *Brucella* strains do not produce this enzyme (22). Consequently, our experimental findings suggest that the *B. abortus* *pykM* mutant is using a pathway known as the “malate shunt,” which relies on the combined activities of PEP carboxykinase, malate dehydrogenase, and the malic enzyme to indirectly convert PEP to pyruvate and sustain carbon flow during carbohydrate metabolism (29, 34). However, it is important to point out here that experimental evidence suggests that *B. abortus* 2308 does not produce a functional PEP

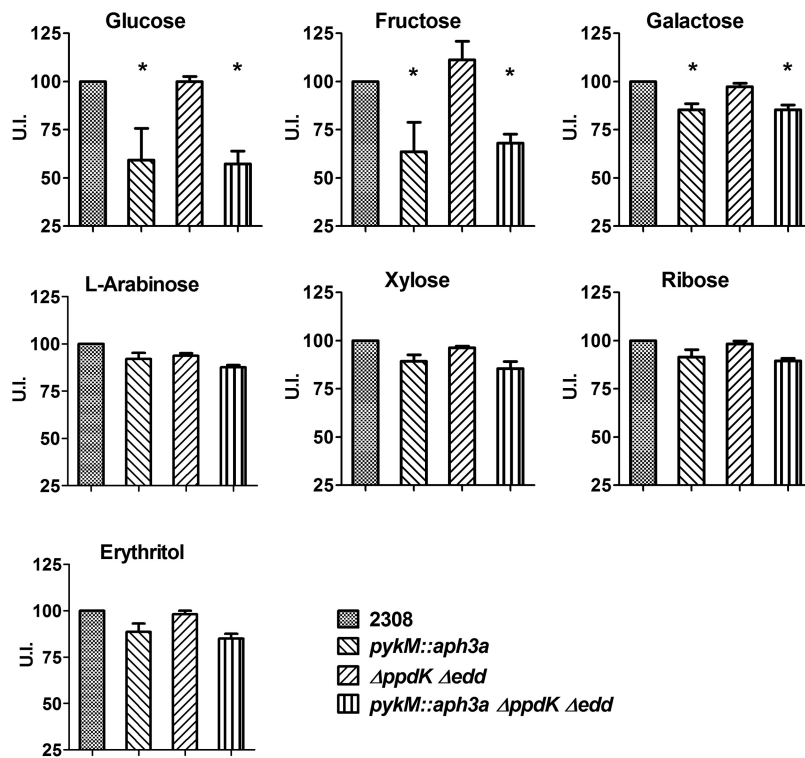


FIG 7 Carbohydrate utilization profiles of *B. abortus* 2308 and isogenic *pykM::aph3a*, $\Delta edd \Delta ppdK$, and *pykM::aph3a \Delta ppdK \Delta edd* mutants. The U.I. was calculated as described in Materials and Methods. The data presented are the means and standard deviations of the results obtained from single determinations made in three different experiments. *, $P < 0.05$ for comparisons of 2308 versus the *pykM::aph3a* and *pykM::aph3a \Delta ppdK \Delta edd* mutants by LSD-ANOVA.

carboxykinase (27, 35); thus, determining how the *B. abortus pykM* mutant converts PEP to pyruvate during carbohydrate catabolism will require further study.

It is presently unclear why the *pykM* mutation only had a negative impact on the capacity of *B. abortus* 2308 to utilize glucose, fructose, and galactose. All three of these sugars are hexoses, and in some bacteria, hexose catabolism via the Entner-Doudoroff (ED) pathway bypasses the need for pyruvate kinase activity (30). Although *Brucella* strains have the genes that encode the enzymes of the ED pathway (22), we found no evidence in these studies that the redirection of hexose catabolism into the ED pathway explains the differential impact that the *pykM* mutation has on the utilization of these hexoses in *B. abortus* 2308. In fact, our data support previous reports that *B. abortus* strains do not use the ED pathway for carbohydrate catabolism (20, 22). On the basis of our results, it seems most likely that the negative impact that the *pykM* mutation has on glucose, fructose, and galactose catabolism in *B. abortus* 2308 is indirect. Glucose-6-phosphate dehydrogenase (Zwf) is required for the entry of these hexoses into the oxidative phase of the pentose phosphate pathway but not for the entry of pentoses or erythritol into the reductive phase of this pathway in *Brucella* (22). Zwf is allosterically inhibited by PEP in the closely related alphaproteobacterium *Caulobacter crescentus* (36); thus, it is conceivable that the intracellular accumulation of this pyruvate kinase substrate in the *B. abortus pykM* mutant has a negative impact on the catabolism of hexoses, but not other carbohydrates, via the pentose phosphate pathway.

PykM and PpdK are both independently required for the wild-type virulence of *B. abortus* 2308 in mice (23, 27), and the enhanced attenuation observed in a mutant lacking both of these enzymes is consistent with these enzymes having different proposed functions in glucose metabolism. These findings also support the proposition put forth by Zúñiga-Ripa et al. (27) that *Brucella* strains rely on the simultaneous catabolism of carbohydrates (e.g., glucose) and amino acids (e.g., gluconeogenic

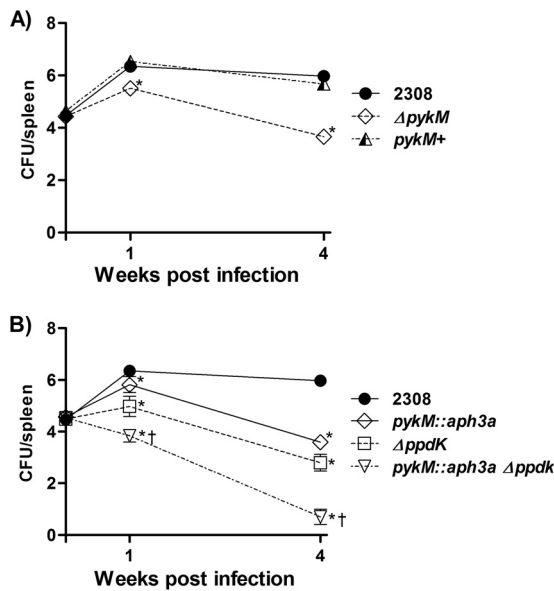


FIG 8 Spleen colonization profiles of *B. abortus* 2308, JEP2 ($\Delta pykM$), and JEP31 ($pykM^+$) (A) and *B. abortus* 2308 and isogenic $pykM::aph3a$, $ppdK$, and $pykM::aph3a ppdK$ mutants (B) in C57BL/6 mice. Five mice were evaluated at each experimental time point for each bacterial strain being examined. *, $P < 0.05$ versus 2308 by one-tailed Student's t test; †, $P < 0.05$ versus $\Delta pykM$ by one-tailed Student's t test.

substrates) to support their intracellular replication in mammalian hosts. From a practical perspective, the independent roles that PykM and PpdK play in the virulence of *B. abortus* 2308 make them both attractive targets for the development of chemotherapeutic agents, and in fact, preliminary studies have shown that some of the bis-indole class of synthetic pyruvate kinase inhibitors (37) have MICs as low as 0.5 $\mu\text{g/ml}$ for *B. abortus* 2308, *B. melitensis* 16M, and *B. suis* 1330 in an *in vitro* assay (J. E. Pitzer, S. Yurist-Doutsch, and E. Dullaghan [Centre for Drug Research and Development], unpublished data).

To the authors' knowledge, the *Bradyrhizobium* and *Brucella* PykM proteins are the only members of this class of pyruvate kinases that have been examined. However, the observation that neither of these enzymes is allosterically regulated by fructose-1,6-bisphosphate (FBP) or AMP is notable. The allosteric regulation of bacterial pyruvate kinases by FBP, AMP, and other metabolic intermediates plays an important role in the capacity of these enzymes to serve as metabolic flux sensors and control carbon flow between catabolic and biosynthetic pathways (38). FBP activation of type I pyruvate kinases, for instance, is thought to be an important "feed forward" mechanism for maintaining carbon flow through the glycolytic pathway (39). Similarly, it has been proposed that the activation of type II pyruvate kinases enables bacteria to adjust their carbon flow toward catabolism when their cellular energy charge is low (40). Although not all bacterial pyruvate kinase are responsive to FBP or AMP, the majority of those that have been characterized are allosterically regulated by one or more metabolic intermediates (41). Hence, it will be important to determine what metabolic intermediates modulate the enzymatic activity of the *Brucella* PykM in order to better understand the role that this enzyme plays in metabolism. Other questions that need to be addressed are whether PykM homologs are the major type of pyruvate kinase found in the alphaproteobacteria in general, and if so, if the distinctive features of this type of pyruvate kinase provide a unique metabolic benefit to these bacteria.

The experimental findings presented here and in previous papers (8, 13) suggest that the high-affinity Mn importer MntH is a critical virulence determinant for *Brucella* strains because it provides these bacteria with sufficient levels of Mn to support their PykM and SodA activities. However, further biochemical and genetic analyses are needed to gain a better understanding of the relative contributions of Mn-dependent

TABLE 1 Bacterial strains and plasmids used in this study

Strain or plasmid	Genotype or description ^a	Reference or source
Strains		
<i>Escherichia coli</i>		
DH5 α	F ⁻ ϕ 80d <i>lacZ</i> Δ M15 Δ (<i>lacZYT-argF</i>)U169 <i>deoR recA1 endA1 hsdR17 phoA supE44 gyrA96 relA1</i>	55
BL21	F ⁻ <i>ompT hsdS_B gal dcm</i>	56
<i>Brucella abortus</i>		
2308	Virulent challenge strain	57
JEP2	2308 Δ <i>pykM</i>	This study
JEP31	JEP2 with a reconstructed wild-type <i>pykM</i>	This study
JEP42	2308 Δ <i>mntH</i>	This study
JEP47	2308 Δ <i>ppdK</i>	This study
JEP79	2308 <i>pykM::aph3a</i> Kan ^r	This study
JEP80	JEP47 <i>pykM::aph3a</i> Kan ^r	This study
JEP81	2308 Δ <i>edd</i>	This study
JEP92	JEP81 <i>pykM::aph3a</i> Kan ^r	This study
JEP93	JEP47 Δ <i>edd</i>	This study
JEP94	JEP93 <i>pykM::aph3a</i> Kan ^r	This study
Plasmids		
pNPTS138	<i>sacB</i> -based gene replacement vector; Kan ^r	58
pGEM-T Easy	Cloning vector; Amp ^r	Promega

^aKan, kanamycin; Amp, ampicillin.

enzymes to the virulence of *Brucella* strains because several other proteins that have been linked to the virulence of *Brucella* strains, such as the (p)ppGpp synthetase/hydrolase Rsh (42), the phosphatidylcholine synthase Pcs (43, 44), and the cyclic di-GMP phosphodiesterases BpdA and BpdB (45), are also likely to be Mn-dependent enzymes based on the biochemical properties of their counterparts in other bacteria (46–48).

MATERIALS AND METHODS

Bacterial strains, plasmids, and culture conditions. A list of the bacterial strains and plasmids used in this study is provided in Table 1. *Brucella abortus* 2308 and the derivatives of this strain were routinely cultivated on Schaedler agar supplemented with 5% defibrinated bovine blood (SBA) at 37°C with 5% CO₂ or in brucella broth at 37°C. When appropriate, the growth media were supplemented with 45 μ g/ml kanamycin or 100 μ g/ml ampicillin to select for plasmid-mediated antibiotic resistance.

The minimal medium described by Gao et al. (23) [yeast extract (1 g/liter), (NH₄)₂SO₄ (13.2 g/liter), Na₂S₂O₃·5H₂O (0.1 g/liter), MgSO₄ (10 mg/liter), MnSO₄ (0.1 mg/liter), NaCl (5 g/liter), KH₂PO₄ (3 g/liter), adjusted to pH 6.8 to 7] and this medium supplemented with 10 g/liter glucose and/or 6 g/liter sodium pyruvate were used to evaluate the capacity of the *B. abortus* strains to grow with glucose as a carbon source. The modified version of Gerhardt's minimal medium (49) described by López-Goñi et al. (50) [yeast extract [0.5 g/liter], lactic acid [4.25 g/liter], glycerol [37.8 g/liter], monosodium glutamate [5 g/liter], NaCl [7.5 g/liter], K₂HPO₄ [10 g/liter], Na₂S₂O₃·5H₂O [0.1 g/liter], adjusted to pH 6.8) served as the base for the Mn-restricted medium used to grow the *B. abortus* strains for the analysis of their cellular pyruvate kinase activity.

Escherichia coli strains DH5 α and BL21 were used as recombinant DNA hosts, and these strains were cultivated on tryptic soy agar at 37°C or in LB broth at 37°C with shaking.

Brucella stock cultures were maintained in brucella broth supplemented with 25% glycerol at –80°C, and *E. coli* stock cultures were maintained in LB supplemented with 25% glycerol at –80°C.

Purification of recombinant *Brucella* pyruvate kinase. The coding region of the *pykM* gene (BAB1_1761) was amplified from *B. abortus* 2308 genomic DNA using PCR and the primers rpykM BamHI F and rpykM HindIII R (Table 2). The amplified DNA fragments were digested with BamHI and HindIII and ligated into BamHI/HindIII-digested pRSET A (Invitrogen). The resulting plasmid was transformed into *E. coli* strain DH5 α and then into BL21. The BL21 strain was grown to an optical density at 600 nm (OD₆₀₀) of approximately 0.6, and recombinant gene expression was induced by the addition of IPTG (isopropyl- β -D-thiogalactopyranoside; 1 mM final concentration). After a 3-h subsequent incubation at 37°C, the bacterial cells were harvested by centrifugation (4,200 \times g for 10 min at 4°C), suspended in 50 mM Tris-HCl (pH 8) containing 0.5 mM phenylmethylsulfonyl fluoride, and lysed by passage through a French pressure cell. Inclusion bodies were then collected from the cell lysate by centrifugation at 10,000 \times g for 10 min at 4°C, followed by serial washing in 50 mM Tris-HCl (pH 8) plus 4% Nonidet P-40 and 50 mM Tris-HCl (pH 8) plus 2 M urea, and a final resuspension in 50 mM Tris-HCl plus 8 M urea. Metals were removed from the protein preparation by adding EDTA to a final concentration of 10 mM and incubating on ice for 30 min. The protein preparation was then dialyzed against 50 mM glycine, 0.005% Tween 20, 10 mM Tris, 100 mM NaH₂PO₄, 5% glycerol, and 2 M urea (pH 7) for 2 h, 10 mM Tris-HCl (pH 8) for 1 h, and then 10 mM Tris-HCl for 30 min at 4°C. Protein concentrations were determined using the Bradford assay, and the purity of the purified protein was assessed by SDS-PAGE.

TABLE 2 Oligonucleotide primers used in this study

Primer	Sequence (5'→3')
PykM up F BamHI	GCAGGATCCTCATCAATAAGACTGCCCG
PykM up R	GGCATTTAGAGCGCATCCCG
PykM down F	TGCGCTTCATTGATTATTCG
PykM down R PstI	GCACTGCAGACAATTGCATGATGAGGGTC
pykM conf F	ATCGATGGTTCAAGTCGAA
pykM conf R	CGCCATGACTGGATGATATT
mntH up F	ATGTCGACCCGGACGTTCCGGAATTCATCGACACT
mntH up R	TACCATATGAAATACCTTTATCCTTTATGCAG
mntH down F	ATTTAAGCACGTTTCCCAGAAAGGGCG
mntH down R	ACGGGGCCCTCTCCCAAGGGCGGTCCAATAAAGAA
mntH conf F	GGCGGATTCGTTCTTCAGTT
mntH conf R	GAAAGGGTGGGGTAAGAGCC
ppdK upF SpeI	GATACTAGTCGCACATGGGTTTTGTCAAGG
ppdK upR	TGCCATTCCGGCCTCCCTTGACACAGGACAAGGTTCCCGAAAG
ppdK downF	GTGTAAACCCTGCTCCATAATTCA
ppdK downR PstI	GATCTGCAGTCTTAGTCGCATTATCTAC
ppdK confF	CTCCGATAAGTCCCATTT
ppdK confR	CGTGAAAACCTTTGAAACATG
edd upF PstI	GATCTGCAGTTGAACGATTGTCATACGG
edd upR	TTCTGAAACAGCGCAATAAATGA
edd downF	GGACATGGGTATCACCTGTGCC
edd downR EcoRI	GATGAATTCATGAGCGCCTCATCATGGATGTGGTGC
edd confF	ATGTGGGTATCAACCGCATC
edd confR	CTTCCTTCTCCCAATGCC
rpykM BamHI F	GGATCCAAGCGCAACCGCAAGGTCAA
rpykM HindIII R	AAGCTTCTAAATGCCGGATTTCCGT

Determination of pyruvate kinase activity and metal cofactor requirements of PykM. The reactions were performed in a 1-ml total volume (25°C, 25 mM Bis-Tris, pH 6.9), and the initial rates were determined using the lactate dehydrogenase (LDH) coupled assay system by monitoring the concomitant reduction of NADH to NAD⁺ at 340 nm spectrophotometrically ($\epsilon_{340 \text{ NADH}} = 6,200 \text{ M}^{-1} \cdot \text{cm}^{-1}$), initiated with the addition of phosphoenolpyruvate (PEP). The reaction mixtures for determining the initial rates as a function of increasing Mg²⁺ or Mn²⁺ concentrations contained 20 mM KCl, 2 mM dithiothreitol (DTT), 2 mM ADP, 2 U LDH (rabbit muscle; Aldrich), 0.15 mM NADH, 2 mM PEP, 50 μg recombinant PykM, and various concentrations of MgCl₂ or MnCl₂ (0 to 3 mM). The specific activity of PykM in the presence of various metals was similarly determined using 10 to 20 mM cationic metal (Zn²⁺, Cu²⁺, Co²⁺, and Fe²⁺). Activities were determined in triplicates, and error bars in the figures are the standard deviations from those separate measurements. Data where MgCl₂ and MnCl₂ were varied were fitted to the Michaelis-Menten equation using nonlinear regression (GraphPad Prism 6.0). The standard errors reported on V_{max} and K_m were determined from that fit.

Pyruvate kinase activity assay in *Brucella* cells. *B. abortus* 2308 and the isogenic *pykM* and *mntH* mutants JEP2 and JEP42, respectively, were grown on SBA for 48 h at 37°C under 5% CO₂. The bacterial cells were harvested from the plates and suspended in 50 ml modified Gerhardt's minimal medium treated with 8-hydroxyquinoline (50), 5 μM FeCl₂, and 0.25 μM MnCl₂ in a 250-ml flask at a cell density of approximately 10⁵ CFU/ml. The cells were incubated with shaking at 37°C until they reached mid-exponential phase (OD₆₀₀ of between 1.0 and 3.0). The bacterial cells were harvested by centrifugation, washed 3 times with 50 mM Tris (pH 8.0), and broken using a BIO101 FastPrep cell disrupter. The total protein concentration of the cell lysate was determined using the Bradford assay. Twenty-five micrograms of cellular protein was added to a reaction mixture containing 25 mM Bis-Tris (pH 6.9), 20 mM KCl, 2 mM dithiothreitol (DTT), 2 mM ADP, 2 IU lactate dehydrogenase (rabbit muscle; Calbiochem), 0.15 mM NADH, and 0.1 mM MnCl₂. The reaction was initiated by adding 2 mM PEP, and the absorbance at 340 nm was measured in a 1-ml cuvette using a Shimadzu UV-1800 spectrophotometer. The background rates of NADH oxidation in the absence of cell lysate or PEP determined in control reactions were subtracted from the final rates determined for the reaction mixtures containing cell lysate and PEP.

Construction of *B. abortus* mutants. Isogenic mutants containing in-frame deletions that fuse the first two codons to the last two codons of the *pykM* (*bab1_1761*), *ppdK* (*bab1_0525*), *edd* (*bab2_0458*), and *mntH* (*bab1_1460*) genes were constructed from *B. abortus* 2308 using the nonpolar unmarked gene excision strategy described by Caswell et al. (51). The gene replacement strategy described by Anderson et al. (52) was also used to construct a derivative of *B. abortus* 2308 in which the *pykM* gene was disrupted by the insertion of the kanamycin resistance gene *aph3a* from pKS-kan (53) 570 nucleotides downstream from the start codon of the *pykM* coding region. The nucleotide primers used for the construction of the pNTPS138- and pGEM-T Easy-based plasmids used for making these mutants are shown in Table 2.

Reconstruction of the parental *pykM* gene in the *B. abortus pykM* null mutant. To confirm the link between the *pykM* mutation and the phenotype exhibited by the *B. abortus pykM* mutant, the strategy described by Elhassanny et al. (54) was used to replace the mutated *pykM* allele in *B. abortus* JEP2

with its wild-type counterpart. The nucleotide primers used to construct the pNTPS138-based plasmid used for this locus reconstruction (PykM up F BamHI and PykM down R PstI) are shown in Table 2, and the *B. abortus* JEP2 derivative with the reconstructed *pykM* locus was given the designation JEP31 (Table 1).

Determination of carbohydrate utilization patterns by the *B. abortus* strains. *B. abortus* strains were grown on SBA for 48 h at 37°C under 5% CO₂, and a loopful of each bacterial culture was spread uniformly across a fresh SBA plate and incubated under these same conditions for 24 h. The bacterial cells were harvested from these plates with a sterile swab and suspended in IF-0a medium to a concentration of 5 × 10¹⁰ CFU per ml. A 1.76-ml volume of this cell suspension was then added to 22.24 ml PM1,2 inoculation fluid, and 100 μl of the resulting mixture was added to each individual well of PM1 and PM2A phenotypic microarray plates (Biolog, Hayward, CA). The plates were incubated for 24 h at 37°C, and the absorbance at 590 nm for each individual well was determined using a Biotek ELx800 microplate reader. These absorbance values were used to calculate a carbohydrate “utilization index” that enabled us to compare the capacity of the each mutant to use a specific carbohydrate against the ability of the parental 2308 strain to use that particular carbohydrate in each individual experiment. This value was calculated by dividing the A₅₉₀ measured for a well containing a specific carbohydrate and mutant by the A₅₉₀ measured for the same carbohydrate and the parental 2308 strain in the same 96-well plate and multiplying by 100.

Virulence of the *B. abortus* mutants in mice. The methods described by Gee et al. (24) were used to evaluate the capacity of the *B. abortus* strains to establish and maintain chronic spleen infections in 4-week-old female C57BL/6 mice (Charles River Labs) infected with 5 × 10⁴ brucellae by the intraperitoneal route. The animal use protocols used for these experiments were reviewed and approved by the East Carolina University Animal Care and Use Committee.

ACKNOWLEDGMENTS

This work was supported by a grant (AI112745) from the National Institute of Allergy and Infectious Disease to R.M.R. and funding from the Brody School of Medicine Division of Research and Graduate Studies to R.M.R., D.W.M., and T.N.Z.

REFERENCES

- Moreno E. 2014. Retrospective and prospective perspectives on zoonotic brucellosis. *Front Microbiol* 5:213. <https://doi.org/10.3389/fmicb.2014.0021>.
- Pappas G, Papadimitriou P, Akritidis N, Christou L, Tsianos EV. 2006. The new global map of human brucellosis. *Lancet Infect Dis* 6:91–99. [https://doi.org/10.1016/S1473-3099\(06\)70382-6](https://doi.org/10.1016/S1473-3099(06)70382-6).
- Roop RM, II. 2012. Metal acquisition and virulence in *Brucella*. *Anim Health Res Rev* 13:10–20. <https://doi.org/10.1017/S1466252312000047>.
- Hood MI, Skaar EP. 2012. Nutritional immunity: transition metals at the pathogen-host interface. *Nat Rev Microbiol* 10:525–537. <https://doi.org/10.1038/nrmicro2836>.
- Hohle TH, O'Brian MR. 2012. Manganese is required for oxidative metabolism in unstressed *Bradyrhizobium japonicum* cells. *Mol Microbiol* 84:766–777. <https://doi.org/10.1111/j.1365-2958.2012.08057.x>.
- Anjem A, Varghese S, Imlay JA. 2009. Manganese import is a key element of the OxyR response to hydrogen peroxide in *Escherichia coli*. *Mol Microbiol* 72:844–858. <https://doi.org/10.1111/j.1365-2958.2009.06699.x>.
- Carlioz A, Touati D. 1986. Isolation of superoxide dismutase mutants in *Escherichia coli*: is superoxide dismutase necessary for aerobic life? *EMBO J* 5:623–630. <https://doi.org/10.1002/j.1460-2075.1986.tb04256.x>.
- Anderson ES, Paulley JT, Gaines JM, Valderas MW, Martin DW, Menscher E, Brown TD, Burns CS, Roop RM, II. 2009. The manganese transporter MntH is a critical virulence determinant for *Brucella abortus* 2308 in experimentally infected mice. *Infect. Immun* 77:3466–3474. <https://doi.org/10.1128/IAI.00444-09>.
- Roop RM, II, Pitzer JE, Baumgartner JE, Martin DW. 2017. Manganese, p 41–61. In Roop RM, II, Caswell CC. (ed), *Metals and the biology and virulence of Brucella*. Springer, Cham, Switzerland.
- Sanders TH, Higuchi K, Brewer CR. 1953. Studies on the nutrition of *Brucella melitensis*. *J Bacteriol* 66:294–299.
- Davies BW, Walker GC. 2007. Disruption of *sitA* compromises *Sinorhizobium meliloti* for manganese uptake required for protection against oxidative stress. *J Bacteriol* 189:2101–2109. <https://doi.org/10.1128/JB.01377-06>.
- Heindl JE, Hibbing ME, Xu J, Natarajan R, Buechlein AM, Fuqua C. 2015. Discrete responses to limitation for iron and manganese in *Agrobacterium tumefaciens*: influence on attachment and biofilm formation. *J Bacteriol* 198:816–829. <https://doi.org/10.1128/JB.00668-15>.
- Martin DW, Baumgartner JE, Gee JM, Anderson ES, Roop RM, II. 2012. SodA is a major metabolic antioxidant in *Brucella abortus* 2308 that plays a significant, but limited, role in the virulence of this strain in the mouse model. *Microbiology* 158:1767–1774. <https://doi.org/10.1099/mic.0.059584-0>.
- Roggenkamp A, Bittner T, Leitritz L, Sing A, Heesemann J. 1997. Contribution of the Mn-cofactored superoxide dismutase (SodA) to the virulence of *Yersinia enterocolitica* serotype O8. *Infect Immun* 65:4705–4710.
- Poyart C, Pellegrini E, Gaillot O, Boumaila C, Baptista M, Trieu-Cuot P. 2001. Contribution of Mn-cofactored superoxide dismutase (SodA) to the virulence of *Streptococcus agalactiae*. *Infect Immun* 69:5098–5106. <https://doi.org/10.1128/IAI.69.8.5098-5106.2001>.
- Esteve-Gassent MD, Elliot NL, Seshu J. 2009. *sodA* is essential for virulence of *Borrelia burgdorferi* in the murine model of Lyme disease. *Mol Microbiol* 71:594–612. <https://doi.org/10.1111/j.1365-2958.2008.06549.x>.
- Kehl-Fie TE, Chitayat S, Hood MI, Damo S, Restrepo N, Garcia C, Munro DA, Chazin WJ, Skaar EP. 2011. Nutrient metal acquisition by calprotectin inhibits bacterial superoxide defense, enhancing neutrophil killing of *Staphylococcus aureus*. *Cell Host Microbe* 10:158–164. <https://doi.org/10.1016/j.chom.2011.07.004>.
- Damo S, Chazin WJ, Skaar EP, Kehl-Fie TE. 2012. Inhibition of bacterial superoxide defense: a new front in the struggle between host and pathogen. *Virulence* 3:325–328. <https://doi.org/10.4161/viru.19635>.
- Xavier MN, Winter MG, Spees AM, den Hartigh AB, Nguyen K, Roux CM, Silva TMA, Atluri VL, Kerrinnes T, Keestra AM, Monack DM, Luciw PA, Eigenheer RA, Bäuml AJ, Santos RL, Tsolis RM. 2013. PPARγ-mediated increase in glucose availability sustains chronic *Brucella abortus* infection in alternatively activated macrophages. *Cell Host Microbe* 14:159–170. <https://doi.org/10.1016/j.chom.2013.07.009>.
- Robertson DC, McCullough WG. 1968. The glucose catabolism of the genus *Brucella*. II. Cell-free studies with *B. abortus* (S-19). *Arch Biochem Biophys* 127:445–456. [https://doi.org/10.1016/0003-9861\(68\)90249-X](https://doi.org/10.1016/0003-9861(68)90249-X).
- Essenberg RC, Seshadri R, Nelson K, Paulsen I. 2002. Sugar metabolism by brucellae. *Vet Microbiol* 90:249–261. [https://doi.org/10.1016/S0378-1135\(02\)00212-2](https://doi.org/10.1016/S0378-1135(02)00212-2).
- Barbier T, Zúñiga-Ripa A, Moussa S, Plovier H, Sternon JF, Lázaro-Antón L, Conde-Álvarez R, De Bolle X, Iriarte M, Moriyón I, Letesson JJ. 2018.

- Brucella* central carbon metabolism: an update. Crit Rev Microbiol 44: 182–211. <https://doi.org/10.1080/1040841X.2017.1332002>.
23. Gao J, Tian M, Bao Y, Li P, Liu J, Ding C, Wang S, Li T, Yu S. 2016. Pyruvate kinase is necessary for *Brucella abortus* full virulence in BALB/c mouse. Vet Res 47:87. <https://doi.org/10.1186/s13567-016-0372-7>.
 24. Gee JM, Valderas MW, Kovach ME, Grippe VK, Robertson GT, Ng W-L, Richardson JM, Winkler ME, Roop RM, II. 2005. The *Brucella abortus* Cu,Zn superoxide dismutase is required for optimal resistance to oxidative killing by murine macrophages and wild-type virulence in experimentally infected mice. Infect Immun 73:2873–2880. <https://doi.org/10.1128/IAI.73.5.2873-2880.2005>.
 25. McCullough NB, Beal GA. 1951. Growth and manometric studies of carbohydrate utilization of *Brucella*. J Infect Dis 89:266–271. <https://doi.org/10.1093/infdis/89.3.266>.
 26. Meyer ME, Cameron HS. 1961. Metabolic characterization of the genus *Brucella*. I. Statistical evaluation of the oxidative rates by which type I of each species can be identified. J Bacteriol 82:387–395.
 27. Zuniga-Ripa A, Barbier T, Conde-Alvarez R, Martinez-Gomez E, Palacios-Chaves L, Gil-Ramirez Y, Grillo MJ, Letesson J-J, Iriarte M, Moriyón I. 2014. *Brucella abortus* depends on pyruvate phosphate dikinase and malic enzyme but not on Fbp and GlpX fructose-1,6-bisphosphatases for full virulence in laboratory models. J Bacteriol 196:3045–3057. <https://doi.org/10.1128/JB.01663-14>.
 28. Raverdy S, Foster JM, Roopenian E, Carlow CKS. 2008. The *Wolbachia* endosymbiont of *Brugia malayi* has an active pyruvate phosphate dikinase. Mol Biochem Parasitol 160:163–166. <https://doi.org/10.1016/j.molbiopara.2008.04.014>.
 29. Olson DG, Hörl M, Fuhrer T, Cui J, Zhou J, Maloney MI, Amador-Noguez D, Tian L, Sauer U, Lynd LR. 2017. Glycolysis without pyruvate kinase in *Clostridium thermocellum*. Metab Eng 39:169–180. <https://doi.org/10.1016/j.ymben.2016.11.011>.
 30. Conway T. 1992. The Entner-Doudoroff pathway: history, physiology and molecular biology. FEMS Microbiol Rev 9:1–28.
 31. Bücken R, Heroven AK, Becker J, Dersch P, Wittmann C. 2014. The pyruvate-tricarboxylic acid node: a focal point of virulence control in the enteric pathogen *Yersinia tuberculosis*. J Biol Chem 289:30114–30132. <https://doi.org/10.1074/jbc.M114.581348>.
 32. Vitko N, Spahich NA, Richardson AR. 2015. Glycolytic dependency of high-level nitric oxide resistance and virulence in *Staphylococcus aureus*. mBio 6:e00045-15 <https://doi.org/10.1128/mBio.00045-15>.
 33. Emmerling M, Dauner M, Ponti A, Fiaux J, Hochuli M, Szyperski T, Wüthrich K, Bailey JE, Sauer U. 2002. Metabolic flux responses to pyruvate kinase knockout in *Escherichia coli*. J Bacteriol 184:152–164. <https://doi.org/10.1128/JB.184.1.152-164.2002>.
 34. Zamboni N, Maaheimo H, Szyperski T, Hohmann H-P, Sauer U. 2004. The phosphoenolpyruvate carboxykinase also catalyzes C₃ carboxylation at the interface of glycolysis and the TCA cycle in *Bacillus subtilis*. Metab Eng 6:277–284. <https://doi.org/10.1016/j.ymben.2004.03.001>.
 35. Zúñiga-Ripa A, Barber T, Lázaro-Antón L, de Miguel MJ, Conde-Álvarez R, Muñoz PM, Letesson JJ, Iriarte M, Moriyón I. 2018. The fast-growing *Brucella suis* biovar 5 depends on phosphoenol pyruvate carboxykinase and pyruvate phosphate dikinase but not on Fbp and GlpX fructose-1,6-bisphosphatases or isocitrate lyase for full virulence in laboratory models. Front Microbiol 9:641. <https://doi.org/10.3389/fmicb.2018.00641>.
 36. Shedlarski JG. 1974. Glucose-6-phosphate dehydrogenase from *Caulobacter crescentus*. Biochim Biophys Acta 358:33–43. [https://doi.org/10.1016/0005-2744\(74\)90255-1](https://doi.org/10.1016/0005-2744(74)90255-1).
 37. Kumar NS, Dullaghan EM, Finlay BB, Gong H, Reiner NE, Jon Paul Selvam J, Thorson LM, Campbell S, Vitko N, Richardson AR, Zoraghi R, Young RN. 2014. Discovery and optimization of a new class of pyruvate kinase inhibitors as potential therapeutics for the treatment of methicillin-resistant *Staphylococcus aureus* infections. Bioorg Med Chem 22: 1708–1725. <https://doi.org/10.1016/j.bmc.2014.01.020>.
 38. Sauer U, Elkmann BJ. 2005. The PEP-pyruvate-oxaloacetate node as the switch point for carbon flux distribution in bacteria. FEMS Microbiol Rev 29:765–794. <https://doi.org/10.1016/j.femsre.2004.11.002>.
 39. Waygood EB, Sanwal BD. 1974. The control of pyruvate kinases of *Escherichia coli*. I. Physicochemical and regulatory properties of the enzyme activated by fructose 1,6-diphosphate. J Biol Chem 249: 265–274.
 40. Garcia-Olalla C, Garrido-Pertierra A. 1987. Purification and kinetic properties of pyruvate kinase isoenzymes of *Salmonella typhimurium*. Biochem J 241:573–581. <https://doi.org/10.1042/bj2410573>.
 41. Donovan KA, Zhu S, Liuni P, Peng F, Kessans SA, Wilson DJ, Dobson RCJ. 2016. Conformational dynamics and allostery in pyruvate kinase. J Biol Chem 291:9244–9256. <https://doi.org/10.1074/jbc.M115.676270>.
 42. Dozot M, Boigegrain RA, Delrue RM, Hallez R, Ouahrani-Bettache S, Danese I, Letesson JJ, De Bolle X, Köhler S. 2006. The stringent response mediator Rsh is required for *Brucella melitensis* and *Brucella suis* virulence, and for expression of the type IV secretion system virB. Cell Microbiol 8:1791–1802. <https://doi.org/10.1111/j.1462-5822.2006.00749.x>.
 43. Comerci DJ, Altabe S, de Mendoza D, Ugalde R. 2006. *Brucella abortus* synthesizes phosphatidylcholine from choline provided by the host. J Bacteriol 188:1929–1934. <https://doi.org/10.1128/JB.188.5.1929-1934.2006>.
 44. Conde-Alvarez R, Grilló MJ, Salcedo SP, de Miguel MJ, Fugier E, Gorvel JP, Moriyón I, Iriarte M. 2006. Synthesis of phosphatidylcholine, a typical eukaryotic phospholipid, is necessary for full virulence of the intracellular bacterial parasite *Brucella abortus*. Cell Microbiol 8:1322–1335. <https://doi.org/10.1111/j.1462-5822.2006.00712.x>.
 45. Petersen E, Chaudhuri P, Gourley C, Harms J, Splitter G. 2011. *Brucella melitensis* cyclic di-GMP phosphodiesterase BpdA controls expression of flagellar genes. J Bacteriol 193:5683–5691. <https://doi.org/10.1128/JB.00428-11>.
 46. Johnson GS, Adler CR, Collins JJ, Court D. 1979. Role of the *spoT* gene product and manganese in the metabolism of guanosine-5'-diphosphate 3'-diphosphate in *Escherichia coli*. J Biol Chem 254: 5483–5487.
 47. Aktas M, Koster S, Kizilirmak S, Casanova JS, Betz H, Fritz C, Moser P, Yildiz O, Narberhaus F. 2014. Enzymatic properties and substrate specificity of a bacterial phosphatidylcholine synthase. FEBS J 281: 3523–3541. <https://doi.org/10.1111/febs.12877>.
 48. Tamayo R, Tischler AD, Camilli A. 2005. The EAL domain protein VieA is a cyclic diguanylate phosphodiesterase. J Biol Chem 280:33324–33330. <https://doi.org/10.1074/jbc.M506500200>.
 49. Gerhart P. 1958. Nutrition of brucellae. Bacteriol Rev 22:81–98.
 50. López-Goñi I, Moriyón I, Neilands JB. 1992. Identification of 2,3-dihydroxybenzoic acid as a *Brucella abortus* siderophore. Infect Immun 60:4496–4503.
 51. Caswell CC, Gaines JM, Roop RM, II. 2012. The RNA chaperone Hfq independently coordinates expression of the VirB type IV secretion system and the LuxR-type regulator BabR in *Brucella abortus* 2308. J Bacteriol 194:3–14. <https://doi.org/10.1128/JB.05623-11>.
 52. Anderson ES, Paulley JT, Martinson DA, Gaines JM, Steele KH, Roop RM, II. 2011. The iron-responsive regulator Irr is required for wild-type expression of the gene encoding the heme transporter BhuA in *Brucella abortus* 2308. J Bacteriol 193:5359–5364. <https://doi.org/10.1128/JB.00372-11>.
 53. Kovach ME, Elzer PH, Hill DS, Robertson GT, Farris MA, Roop RM, II, Peterson KM. 1995. Four new derivatives of the broad-host-range cloning vector pBBR1MCS, carrying different antibiotic-resistance cassettes. Gene 166:175–176. [https://doi.org/10.1016/0378-1119\(95\)00584-1](https://doi.org/10.1016/0378-1119(95)00584-1).
 54. Elhassanny AEM, Anderson ES, Menscher EA, Roop RM, II. 2013. The ferrous iron transporter FtrABCD is required for the virulence of *Brucella abortus* 2308 in mice. Mol Microbiol 88:1070–1082. <https://doi.org/10.1111/mmi.12242>.
 55. Hanahan D, Jessee J, Bloom FR. 1991. Plasmid transformation of *Escherichia coli* and other bacteria. Methods Enzymol 204:63–113. [https://doi.org/10.1016/0076-6879\(91\)04006-A](https://doi.org/10.1016/0076-6879(91)04006-A).
 56. Studier FW, Moffatt BA. 1986. Use of bacteriophage T7 RNA polymerase to direct selective high-level expression of cloned genes. J Mol Biol 189:113–130. [https://doi.org/10.1016/0022-2836\(86\)90385-2](https://doi.org/10.1016/0022-2836(86)90385-2).
 57. Jones LM, Montgomery V, Wilson JB. 1965. Characteristics of carbon dioxide-independent cultures of *Brucella abortus* isolated from cattle vaccinated with Strain 19. J Infect Dis 115:312–320. <https://doi.org/10.1093/infdis/115.3.312>.
 58. West L, Yang D, Stephens C. 2002. Use of *Caulobacter crescentus* genome sequence to develop a method for systematic genetic mapping. J Bacteriol 184:2155–2166. <https://doi.org/10.1128/JB.184.8.2155-2166.2002>.